**Proceedings of the ASME 2010 3rd Joint US-European Fluids Engineering Summer Meeting and 8th International Conference on Nanochannels, Microchannels, and Minichannels**
**FEDSM-ICNMM2010**
**August 1-5, 2010, Montreal, Canada**

# FEDSM-ICNMM2010-30716

# ANALYSIS OF THE DRAG REDUCTION USING VORTEX KINEMATICS BEHIND A BLUFF BODY

**Charles-Henri Bruneau**
IMB Université de Bordeaux
$MC^2$ INRIA Bordeaux Sud-Ouest
351, cours de la Libération
F-33405 Talence FRANCE
bruneau@math.u-bordeaux1.fr

**Emmanuel Creusé**
Laboratoire Paul Painlevé
SIMPAF INRIA Lille Nord Europe
UST Lille
F-59655 Villeneuve d'Ascq FRANCE
creuse@math.univ-lille1.fr

**Delphine Depeyras**
IMB Université de Bordeaux
$MC^2$ INRIA Bordeaux Sud-Ouest
351, cours de la Libération
F-33405 Talence FRANCE
delphine.depeyras@math.u-bordeaux1.fr

**Patrick Gilliéron**
Direction de la recherche
RENAULT - DREAM/DTAA
1, Avenue du Golf
F-78288 Guyancourt FRANCE
patrick.gillieron@renault.com

**Iraj Mortazavi**
IMB Université de Bordeaux
$MC^2$ INRIA Bordeaux Sud-Ouest
351, cours de la Libération
F-33405 Talence FRANCE
mortaz@math.u-bordeaux1.fr

## ABSTRACT

The aim of this work is to analyse one of the mechanisms that contributes to the drag forces, namely the distance of the vortices to the back wall of a bluff body. The study shows the strong relationship between this distance and the pressure forces at the back. Indeed, the active control processes modify the trajectory of the vortices to accelerate their removal from the wall and consequently reduce the drag coefficient.

## NOMENCLATURE

U=(u,v), p velocity field and pressure

Re non dimensional Reynolds number

K non dimensional permeability coefficient of the medium

H height of the Ahmed body

$\Gamma$ Vortex circulation

$F_p$ pressure force

$C_d$ drag coefficient

## INTRODUCTION

A large part of the drag coefficient around a bluff body is due to the pressure forces on the front and back walls. In particular the vortices generated on the sharp corners of the geometry are moved in the near wake, inducing strong pressure forces at the back. Consequently, each time a big vortex stand close to the wall the drag coefficient increases. A way to reduce this drag coefficient is to control the flow so that the vortices are either smaller or convected away faster. To reduce the size of the vortices, one way is to use porous slices to create a low speed flow parallel to the main flow [Bruneau and Mortazavi 2004, Bruneau et al. 2008]. Then Kelvin-Helmholtz instabilities generate small eddies that are less strong and the pressure forces are reduced.
To convey faster the vortices, active control using blowing jets can be an efficient tool [Brunn et al. 2007, Rouméas 2006]. In this work, the bluff body is a simplified car called the square-back Ahmed body [Ahmed et al. 1984]. A theoretical study shows the strong relationship between the distance of an inviscid vortex and the pressure forces on the back wall. Then, the results given by the active control process are analysed to prove that this

relationship is true in a real flow. Indeed, the variations of the drag coefficient are directly linked to the distance of the strong shedding vortices to the back wall. This paper is organized as follows: for some removal analytical functions, the corresponding forces are computed, then a study is performed using a vortex superimposed on a given background flow. Finally, the study of the trajectories of the vortices in the vicinity of the back wall for some real flows, shows the impact of the distance of the vortices to the pressure drag forces and thus on the whole drag coefficient.

## 1 ANALYTICAL APPROACH

Using the mirror image vortex theory [Lamb 1916], the sliding forces of a vortex at the wall are the amount of the forces generated by the studied vortex and its wall mirror image vortex. Let $H$ be the height of the back wall of the obstacle characterized by the coordinates set $x = 0$ and $-H/2 \leq z \leq H/2$ (see Figure 1). Let us consider $M(0,z)$ a point on the back wall and a vortex whose center is located at point $P(x_1,z_1)$, $x_1 \geq 0$. The distance between $M$ and $P$ is denoted $d$, and $\vec{\tau}_{MP}$ is the unit vector given by $\vec{\tau}_{MP} = \vec{MP}/||\vec{MP}||$. In that case, according to [Milne-Thomson

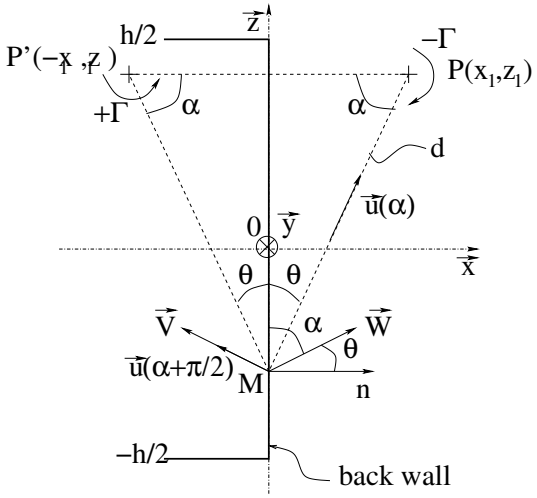


Figure 1: Location of the vortex center P respecting to the infinitesimal surface M of the wall.

1966], the wall velocity induced at point $M$ by the vortex is given by

$$\vec{V}(M) = \frac{\Gamma}{2\pi d}\,\vec{\tau}_{MP},$$

where $-\Gamma \in \mathbb{R}$ corresponds to the vortex circulation. Let the mirror image vortex be located at the point $P'(-x_1,z_1)$ with circulation $+\Gamma$, The velocity $\vec{W}(M)$ at point $M$ due to this mirror image vortex can be defined the same way and a simple calculation shows that the modulus of the resulting velocity $\vec{V_R}(M) = \vec{V}(M) + \vec{W}(M)$ is given by

$$V_R(M) = ||\vec{V_R}(M)|| = \frac{\Gamma\, x_1}{\pi(x_1^2 + (z-z_1)^2)}.$$

When $x$ goes towards infinity, the velocity $V_R(M)$ does also and, according to Bernoulli, the local pressure $p$ with respect to the pressure at rest $p_0$ is given by

$$p(M) - p_0 = -\frac{\rho}{2} V_R^2(M) = -\frac{\rho}{2}\frac{\Gamma^2\, x_1^2}{\pi^2(x_1^2 + (z-z_1)^2)^2}.$$

Consequently, integrating on the back wall, we get the horizontal pressure force $F_p$ induced by the vortex on the whole back of the body and, considering that the vortex is moving, the instantaneous pressure force $F_p(t)$ induced by the vortex on the wall at

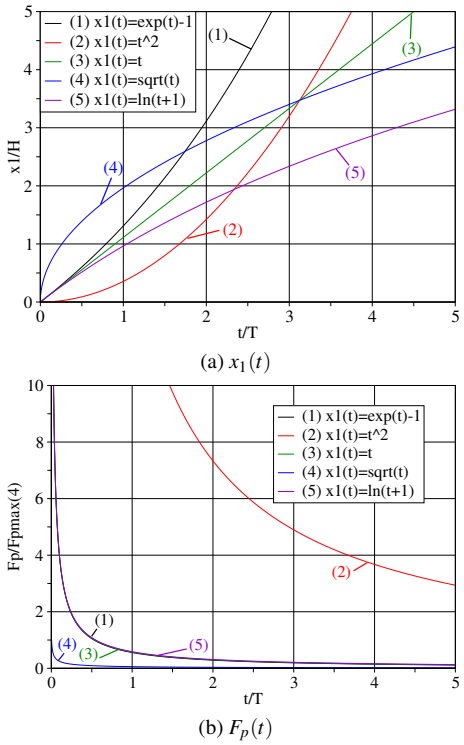


(a) $x_1(t)$

(b) $F_p(t)$

Figure 2: Vortex evolutions and corresponding pressure forces.

time $t$ is:

$$F_p(t) = \frac{\rho}{2}\frac{\Gamma^2}{\pi^2}\int_{-\frac{H}{2}}^{+\frac{H}{2}} \frac{x_1^2(t)}{(x_1^2(t)+(z-z_1(t))^2)^2}dz.$$

This pressure force depends of course strongly on the function $x_1(t)$. Taking $x_1(t) = t^r$ with $1/2 \leq r \leq 2$, $x_1(t) = exp(t) - 1$ or $x_1(t) = Ln(t+1)$ (see [Milne-Thomson 1966]), and considering in a first approach an horizontal evolution ($z_1(t) \equiv 0$), some characteristic behaviours of the vortex trajectories behind the back wall can be represented. In Figure 2 are represented these functions $x_1(t)$ and the corresponding pressure forces $F_p(t)$. The best result (the lowest pressure force) is achieved for $r = 1/2$ as it corresponds to the fastest removal from the wall at $t = 0$.

## 2 MODELING AND NUMERICAL SIMULATION

To simulate the flow around the square back Ahmed body with height $H = 1$, the penalized Navier-Sokes equations (see [Angot et al. 1999, Bruneau and Mortazavi 2008]) are solved for the genuine unknowns velocity and pressure $(U, p)$ in the two-dimensional computational domain $\Omega = (0, 15H) \times (0, 5H)$ with the body located at the distance 0.6 from the road (Figure 3) and whose length is $L = 3.625$:

$$\partial_t U + (U \cdot \nabla)U - \frac{1}{Re}\Delta U + \frac{U}{K} + \nabla p = 0 \;\; in\; \Omega_T = \Omega \times (0,T),$$
$$div U = 0 \;\; in\; \Omega_T,$$

where $T$ is the simulation time, $K = \frac{\rho k \Phi \overline{U}}{\mu H}$ is the non dimensional coefficient of permeability of the medium, $k$ is the intrinsic permeability, $\mu$ is the viscosity, $\Phi$ is the porosity of the fluid and $Re$ is the Reynolds number. The simulations are performed in two-dimensions as it has been shown that for this body the flow has almost a two-dimensional behaviour [Krajnović and Davidson 2003, Gilliéron and Chometon 1999]. To recover the genuine Navier-Stokes equations we set $K = 10^{16}$ in the fluid. On the contrary, setting $K = 10^{-8}$ in the solid body mimics a porous body with a very low permeability and thus the velocity field is also of $10^{-8}$ order inside the body. These values of $K$ are set on the staggered velocity points of a Cartesian mesh according to their location. The equations are coupled to an initial datum corresponding to the flow at rest and to two kinds of boundary conditions. A constant Dirichlet condition upstream and on the road $\overline{U} = (1,0)$ corresponding to the speed of the ground vehicle and a non reflecting boundary condition on the open frontiers (top and downstream) [Bruneau 2000].
The time discretization is achieved using a second-order Gear scheme with explicit treatment of the convection term. All the linear terms are treated implicitly and discretized via a second-order centered finite differences scheme. A third-order finite differences upwind scheme is used for the discretization of the convection terms [Bruneau and Saad 2006]. The efficiency of the resolution is obtained by a multigrid procedure using a cell-by-cell relaxation smoother.
The results are presented at $Re = 30,000$ based on the body length on a $1920 \times 640$ cells uniform mesh that insures that grid convergence is reached.

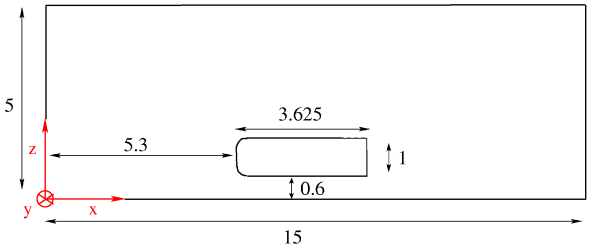


Figure 3: Computational domain around the square back Ahmed body.

## 3 KINEMATICS AND CONTROL OF AN ANALYTICAL VORTEX

The real wake behind a bluff body is composed of vortical structures with different circulations and periods of shedding depending on the geometrical constraints and the Reynolds number. They have a mutual interaction with the near wake flow feeding the vortex street generation and being themselves conditioned by the former generated vortices. However, even if this high order real motion topology is very complex, its main characteristics can be mimicked by simplified kinematic verifications based on the vortex trajectories and their speed of removal from the wall [Sipp et al. 1999]. Previous studies have shown that the flow behind a bluff-body can be divided into two main areas: the vortex formation area (near wake) and the transport area [Mortazavi and Giovannini 2001]. In this section, in order to better understand the effect of the shedding vortices on the body forces, the formation zone kinematics is analyzed and connected to simplified inviscid models. Then, the results are applied to a constant blowing active control technique in order to explain its efficiency to reduce the drag coefficient.
For a first approach, the typical trajectory of a circular vortex [Batchelor 1967] with a linear velocity distribution inside the vortex in an instantaneous flow wake around the Ahmed body without and with control is computed (Figure 4):

$$u_{flow+vortex} = u_{flow} - C\,\frac{z-z_0}{2R_0}\,e^{-\left(\frac{R}{R_0}\right)^2},$$

$$v_{flow+vortex} = v_{flow} + C\,\frac{x-x_0}{2R_0}\,e^{-\left(\frac{R}{R_0}\right)^2},$$

where $(x_0, z_0)$ is the vortex center, $R$ is the distance between the studied points of the domain and the vortex center and $R_0 = 0.05$ the viscous radius of the vortex. The velocity is zero in the centre and increases linearly with the radius. When this radius is upper than the viscous radius, the velocity decreases with the opposite of the radius towards zero far away of the vortex center (Figure 5).

To have a proportional dimension to shedding vortices, the theoretical vortex is initially defined with $C = 2$. The initial condition for the flow field is chosen when the upper near wake is almost vortex free, then the theoretical vortex will shed at the beginning of a new period. The initial position of the vortex center is $(9.02, 1.56)$ (see Figure 3), corresponding to the appearance of any new shedding in the upper edge of the obstacle for the uncontrolled mean flow. The study focuses on the comparison of the trajectories of this vortex in the near wake for both uncontrolled and controlled (with a steady jet) flows. For the steady active control, the actuator with the amplitude of $U_j = 0.6U_0$, is located at $H/3$ from the upper edge of the back wall. On the Figure 6 the trajectory $(a)$ and the removal speed $(b)$ of the theoretical vortex for both uncontrolled and controlled cases are compared. In the Figure 6 $(a)$, the letters $A$ to $F$ correspond to definite times on the trajectories of the vortex for both flows (Table 1). The trajectory plot shows that as soon as the vortex attends the front point of the control jet, its motion is considerably modified and accelerated inside the wake compared to the uncontrolled case. At the same time, the pressure force on the wall generated by this vortex looses its effect much more quickly than without the blowing jet. This acceleration and pushing property are also well demonstrated in the Figure 6 $(b)$, where the controlled curve comes closer to the linear motion which corresponds to a smaller pressure force on the back wall. So, we can expect to use this mechanism on real shedding of vortices behind obstacles.

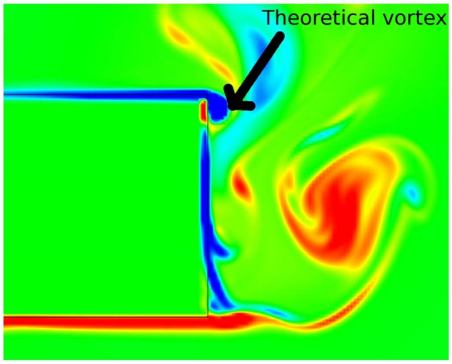


Figure 4: Initial instantaneous flow for the theoretical vortex study.

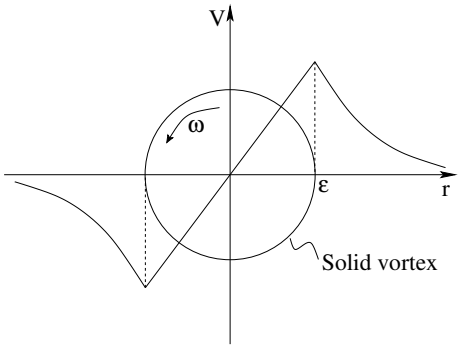


Figure 5: Velocity vs radius for a circular vortex [Milne-Thomson 1966].

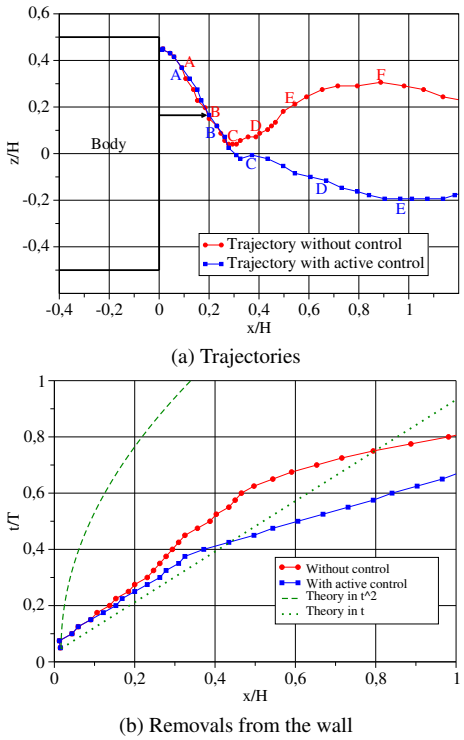


(a) Trajectories

(b) Removals from the wall

Figure 6: Comparison of trajectories and removals from the wall for the theoretical vortex in an instantaneous flow.

| Points | $A$ | $B$ | $C$ | $D$ | $E$ | $F$ | $G$ | $H$ |
|---|---|---|---|---|---|---|---|---|
| Time $t$ | 0.5 | 1.0 | 1.5 | 2.0 | 2.5 | 3.0 | 3.5 | 4.0 |

Table 1: The letters show the simulation time since the origin of the trajectory.

## 4 KINEMATICS AND CONTROL OF A REAL FLOW

Starting from the same initial solution in both cases, the flow without control is compared to the controlled flow with the actuator in the middle of the back wall. This position is chosen in order to take into account the shedding of vortices on both sides of the back wall.

To get a general view of the relationship between vortex kinematics and the drag reduction due to the control, an averaged estimation of several vortex motions is performed and the mean trajectories of the up and down vortices are studied. The averaging procedure is performed for 10 successive vortices on both sides of the wall from $t = 3.0$ until $t = 23.0$. In the Figure 7 the mean uncontrolled trajectories are compared to the mean controlled ones. As the figure shows, the trajectories are about the same for the upper shedding processes. but, the lower trajectories are drastically modified as the vortices are expelled from the body much more quickly with the control. In the Figure 8, for the upper vortex, the uncontrolled and controlled cases are very similar and show almost a linear behaviour $(a)$. While, for the lower shedding the uncontrolled case is removed from the wall with a polynomial law close to $t^2$ whereas for the controlled case, the removal procedure is much more accelerated and is defined by a linear law with a smaller slope compared to the linear motion $t$ $(b)$. Let us note that the active control induces a strong pressure forces reduction at the back and consequently a 20% reduction of the whole drag coefficient $C_d$. This result shows the efficiency of the active control on the lower shedding process. The difference between the upper and lower sheddings is due to the presence of the road as the jet flow under the body enhances the control jet effect. It is thus possible to connect the control efficiency to the removal speed of the vortices from the wall.

## 5 CONCLUSIONS

In the first part of this paper, the drag effect of a theoretical vortex moving away from a wall with analytical laws is studied. It is shown that the magnitude of wall pressure forces on the back wall depends directly on the removal speed of the vortex. The more this speed is large, the more the pressure forces decrease. An active control by a blowing jet in front of an analytical vortex in a real flow changes the trajectory and accelerates the removal speed of the vortex.

Then, the study of a real flow around a square back Ahmed body on top of a road shows that a blowing jet accelerates the removal of the vortices from the wall inducing a strong decrease of the pressure forces at the back and consequently a 20% decrease of the drag coefficient.

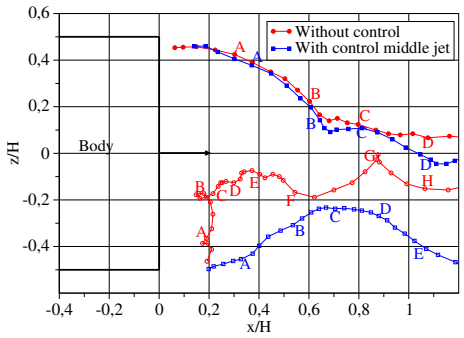


Figure 7: Comparison of averaged trajectories of the vortices for the cases without control and with an active control in the middle of the wall, for a real flow.

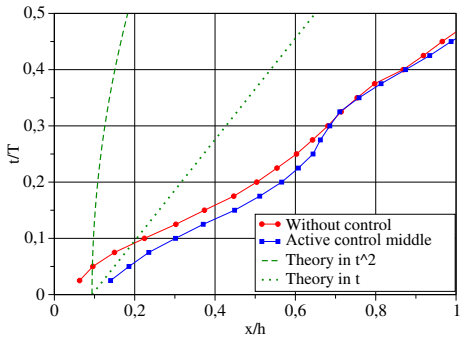


(a) Up

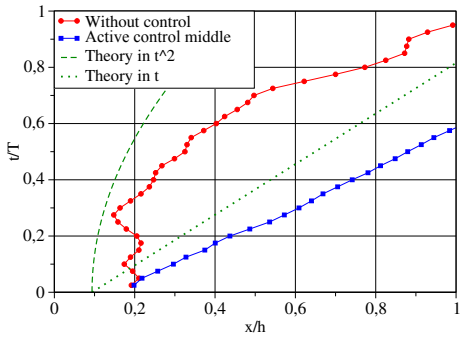


(b) Down

Figure 8: Comparison of averaged removals of the vortices from the wall for the cases without control and with an active control in the middle of the wall, for a real flow.

## REFERENCES


[Ahmed et al. 1984] Ahmed S. R., Ramm G., Faltin G., *Some Salient Features of the Time -Averaged Ground Vehicle Wake*, SAE-Paper **840300**, 1984.

[Angot et al. 1999] Angot Ph., Bruneau Ch.-H., Fabrie P., *A penalization method to take into account obstacles in incompressible viscous flows*, Numer. Math. **81**, 1999.

[Batchelor 1967] Batchelor G. K., *An Introduction to Fluid Dynamics*, Cambridge University Press, 1967.

[Bruneau 2000] Bruneau Ch.-H., *Boundary conditions on artificial frontiers for incompressible and compressible Navier-Stokes equations*, Math. Model. Num. Anal. **34** (2), 2000.

[Bruneau and Mortazavi 2004] Bruneau Ch.-H., Mortazavi I., *Passive control of bluff body flows using porous media*, Int. J. for Num. Meth. in Fluids **46**, 2004.

[Bruneau and Mortazavi 2008] Bruneau Ch.-H., Mortazavi I., *Numerical modelling and passive flow control using porous media*, Computers & Fluids **37**, $n^0$ 5, 2008.

[Bruneau et al. 2008] Bruneau Ch.-H., Mortazavi I., Gilliéron P., *Passive control around the two-dimensional square back Ahmed body using porous devices*, J. Fluids Eng. **130**, 2008.

[Bruneau and Saad 2006] Bruneau Ch.-H., Saad M., *The 2D Lid-driven cavity problem revisited*, Computers & Fluids **35**, $n^0$ 3, 2006.

[Brunn et al. 2007] Brunn A., Wassen E., Sperber D., Nitsche W., Thiele F., *Active Drag Control for a Generic Car Model*, King (ed.) Active Flow Control, Notes on Numerical Fluid Mechanics and Multidisciplinary Design **95**, 247-259, 2007.

[Gilliéron and Chometon 1999] Gilliéron P., Chometon P., *Modelling of Stationary Three-Dimensional Separated Air Flows around an Ahmed Reference Model*, ESAIM **7**, 1999.

[Krajnović and Davidson 2003] Krajnović S., Davidson L., *Numerical study of the flow around the bus-shaped body*, ASME J. Fluids Eng. **125**, 2003.

[Lamb 1916] Lamb H., *Hydrodynamics*, Cambridge University Press, 1916.

[Milne-Thomson 1966] Milne-Thomson L.M., *Theoretical aerodynamics*, Dover, 1966.

[Mortazavi and Giovannini 2001] Mortazavi I., Giovannini A., *The Simulation of Vortex Dynamics downstream of a Plate Separator using a Vortex-Finite Element Method*, Int. J. Fluid Dyn. **vol. 5**, 2001.

[Rouméas 2006] Rouméas M., *Contribution à l'analyse et au contrôle des sillages de corps épais par aspiration ou soufflage continu*, Ph D thesis Toulouse, France, 2006.

[Sipp et al. 1999] Sipp D., Coppens F., Jacquin L., *Theoretical and numerical analysis of wake vortices*, ESAIM Proceedings, **7**, 1999.